Fe_3O_4 thin films sputter deposited from iron oxide targets

Yingguo Peng[a)]
Data Storage Systems Center, Carnegie Mellon University, Pittsburgh, Pennsylvania 15213 and Electrical and Computer Engineering Department, Carnegie Mellon University, Pittsburgh, Pennsylvania 15213

Chando Park
Data Storage Systems Center, Carnegie Mellon University, Pittsburgh, Pennsylvania 15213 and Materials Science and Engineering Department, Carnegie Mellon University, Pittsburgh, Pennsylvania 15213

David E. Laughlin
Data Storage Systems Center, Carnegie Mellon University, Pittsburgh, Pennsylvania 15213; Electrical and Computer Engineering Department, Carnegie Mellon University, Pittsburgh, Pennsylvania 15213; and Materials Science and Engineering Department, Carnegie Mellon University, Pittsburgh, Pennsylvania 15213

(Presented on 14 November 2002)

Fe_3O_4 thin films have been directly sputter deposited from a target consisting of a mixture of Fe_3O_4 and Fe_2O_3 onto Si and glass substrates. The magnetic properties and microstructures of the films have been characterized and correlated. The columnar growth of the Fe_3O_4 grains was found to be initialized from the substrate surface without any critical thickness. Substrate bias was found to be a very effective means of improving the crystal quality and magnetic properties of the thin films. The crystallographic defects revealed by high resolution transmission electron microscopy seem to be a characteristic of the films prepared by this method. © *2003 American Institute of Physics.*
[DOI: 10.1063/1.1556252]

I. INTRODUCTION

Due to the predicted half-metallic nature and high polarization (100%), Fe_3O_4 thin films have drawn a great deal of interest as promising candidates for application in tunneling magnetoresistance (TMR) devices. Single crystalline thin films have been epitaxially grown on MgO(100) substrates, due to the good lattice match between the oxides.[1–3] Polycrystalline Fe_3O_4 thin films have also been deposited on Si substrates to study the properties.[4,5] The deposition methods used to date include plasma assisted molecular-beam epitaxy (MBE),[1] pulsed laser deposition (PLD) from oxide targets,[2,4] and reactive sputter deposition from an Fe target with Ar–O_2 mixture gas flow.[3,5] Besides Fe_3O_4, other iron oxides, Fe_2O_3, FeO, and some nonstoichiometric oxides, have been reported to be present in the deposited films, depending on the deposition conditions.[6,7] Fe_2O_3 is brown or reddish brown and hence can be easily distinguished from the other oxides, FeO and Fe_3O_4, which are black. The crystal structure of both of the later oxides are based on the fcc Bravias Lattice with lattice parameters $a = 0.8936$ nm for Fe_3O_4 and 0.4307 nm for FeO. It has been reported that Fe_3O_4 can be obtained in polycrystalline thin films only after a certain critical thickness has been deposited,[8] which is not ideal for practical device applications. Here we report our investigations of the deposition of Fe_3O_4 thin films rf sputtered from an iron oxide target.

[a)]Electronic mail: yingguo@ece.cmu.edu

II. EXPERIMENT

Iron oxide films were rf-sputter deposited onto Si and glass substrates from a target that consisted of Fe_3O_4 and Fe_2O_3 in a Z-400 sputtering system. The base pressure in the chamber before sputtering was $(4-6)\times 10^{-7}$ Torr. During sputtering, the bleeding pressure was set to 10, 50, and 100 mTorr, and the rf power was 100, 200, or 300 W. Substrate bias was also applied for the different combinations of bleeding pressure and rf power. The magnetic hysteresis loops were taken from the sputtered thin films with an alternating gradient magnetometer (AGM) and a superconducting quantum inference device (SQUID). X-ray spectra of conventional θ–2θ as well as glancing angle scans were collected to identify the phases. Surface roughness was measured with an atomic force microscope (AFM). Microstructures were investigated with a Tecnai F20 and a JEM-2010 transmission electron microscope (TEM).

III. RESULTS AND DISCUSSION

The x-ray diffraction pattern of the iron oxide target is shown in Fig. 1. All the peaks can be indexed as either Fe_3O_4 or Fe_2O_3. The target is estimated to be 50% Fe_3O_4 and 50% Fe_2O_3. An Fe_2O_3 target has been used in PLD to deposit Fe_3O_4 thin films,[3] which implies that there is a loss of oxygen upon deposition. It was expected that the addition of Fe_2O_3 to Fe_3O_4, which has a higher content of oxygen, helps to balance the stoichiometry in our deposition. By control of the sputtering power and chamber pressure, different types of iron oxides or mixtures of the oxides were obtained on either the Si or glass substrates. Glass substrates are used

 © 2003 American Institute of Physics

Downloaded 23 May 2003 to 128.2.132.216. Redistribution subject to AIP license or copyright, see http://ojps.aip.org/japo/japcr.jsp

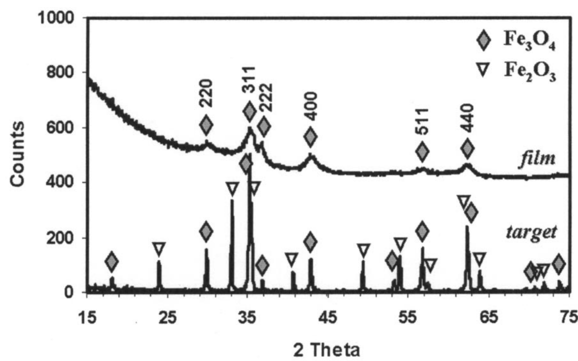

FIG. 1. X-ray spectra of the iron oxide target (θ–2θ scan) and the sputtered Fe_3O_4 thin film (glancing angle scan).

to reveal the color and rule out the Fe_2O_3 films without x-ray diffraction. Si substrates are used for the samples prepared for TEM studies. It was found that the plasma power has a greater impact on the type of the oxides formed than does the chamber pressure. Sputtering at 10, 50, and 100 mTorr did not result in a great difference in the color or of the x-ray spectra of the films. However, Fe_2O_3 is the dominant phase in the thin films at a lower sputtering power of 100 W, while FeO (determined by x-ray diffraction) is dominant in the films sputtered at a higher power of 300 W. Thin films sputtered at 200 W were found to be Fe_3O_4 by x-ray (Fig. 1) and electron diffraction [Fig. 2(a)]. In Fig. 1, the spectrum of the thin film was collected at glancing angle configuration for a higher intensity, for which it is prerequisite that the film does not have any texture. The profile of the intensity integrated along the radius shown in Fig. 2(b) is generated with a computer program developed by Labar.[9] All the peaks fit well with Fe_3O_4. No other phases have been detected from the thin film either by x-ray diffraction (Fig. 1) which averages a large area or by selected area electron diffraction (Fig. 2) that is produced within a local region of the film.

Substrate bias was also applied during sputtering. Fe_3O_4 films were obtained at 100 W for the films when a bias was present which was expected since bias usually increases the content of heavier atoms in the films. The films produced without bias at 100 W were mainly Fe_2O_3. The comparison of the magnetic properties and microstructures showed that 100 V substrate bias resulted in a significant improvement in the thin film quality. Table I summarizes some of the important physical properties of thin films sputtered with and without substrate bias.

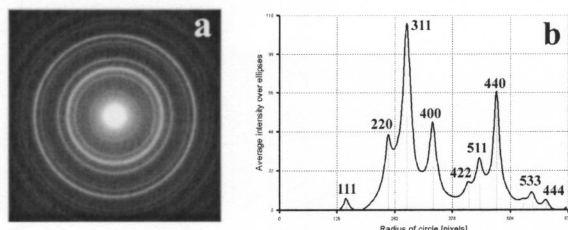

FIG. 2. Selected area electron diffraction pattern (a) and the intensity profile around the radius direction (b) of the sputtered Fe_3O_4 thin film.

TABLE I. Some physical properties of Fe_3O_4 thin film sputtered with and without substrate bias.

	$(10^{-4}\ \Omega\text{m})$	R_a/R_q (nm)	H_c (Oe)	M_s (emu/cc)
100 V biased	2.98	0.84/1.05	300	212
Nonbiased	19.9	2.27/2.95	127	109

The electrical resistivity ρ was measured at room temperature by a dc four-probe method from $5\times1\ \text{mm}^2$ samples. Both the biased and nonbiased films have a resistivity value that is greater than that of well characterized single crystals [typically $<10^{-5}\ \Omega$ m (Ref. 10)], but the values are normal for polycrystalline thin films [$3.5\times10^{-4}\ \Omega$ m (Ref. 5)]. However, the improvement in resistivity by applying substrate bias is apparent, nearly one order of magnitude. Figure 3 represents the TEM plan-view images of the two films. It is noted that the image contrast of the biased sample is similar with that of Fe_3O_4 thin films sputtered by other methods.[3,8] However, the grain boundaries in the nonbiased thin film are much thicker and less dense, and the density of defects is higher as well. It is believed that the boundary region is amorphous and may also contain some voids, which would of course increase the electrical resistivity of the thin film.

Surface roughness is a critical factor to the practical device applications. AFM images are employed for this measurement. The average roughness of a 170 nm film was measured to be less than 1 nm. The TEM cross-section image shown in Fig. 4 also shows a smooth surface of the film. It can be also seen from Fig. 4(a) that the Fe_3O_4 columnar grains grow right from the substrate surface. There are no other phases formed at the beginning stage of sputtering. In other words, the microstructure of the thin films is homogeneous through the whole thickness and hence the properties are expected to be independent of the thickness.

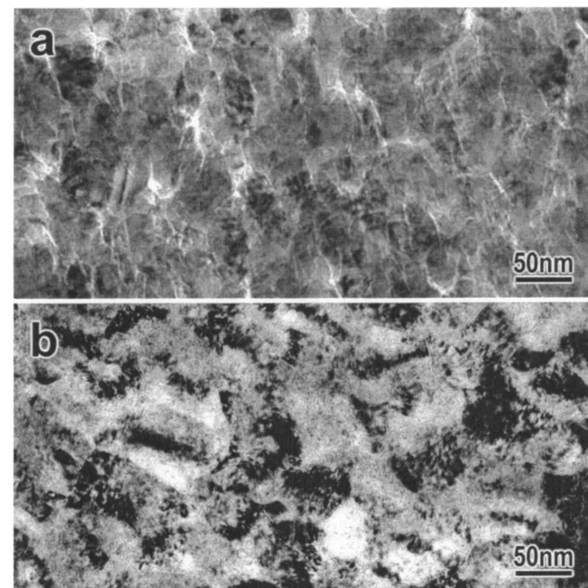

FIG. 3. Plan-view TEM images of the Fe_3O_4 thin film sputtered without substrate bias (a) and that with 100 V bias (b)

Downloaded 23 May 2003 to 128.2.132.216. Redistribution subject to AIP license or copyright, see http://ojps.aip.org/japo/japcr.jsp

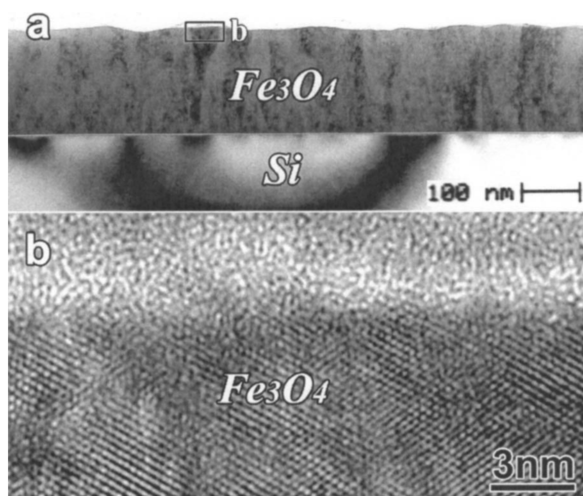

FIG. 4. Cross-sectional TEM image showing the columnar grains (a) and high resolution image showing the flat and smooth surface (b) of Fe_3O_4 thin film.

Figure 5 represents the AGM hysteresis loops of the Fe_3O_4 thin films sputtered with and without substrate bias, from which the values of H_c and M_s are measured. SQUID was also employed to obtain a more accurate value of M_s. Substrate bias has increased both the coercivity and saturation magnetization about two times. This is possibly due to that the bias has removed the grain boundary phase, which is probably nonmagnetic, and improved the crystal quality by reducing defects density. The H_c value of the Fe_3O_4 film sputtered with substrate bias lies in the normal range for Fe_3O_4 films. However, the M_s value is still below that of the well characterized Fe_3O_4 thin films, i.e., >400 emu/cc.[4] The high resolution TEM image shown in Fig. 6 reveals many

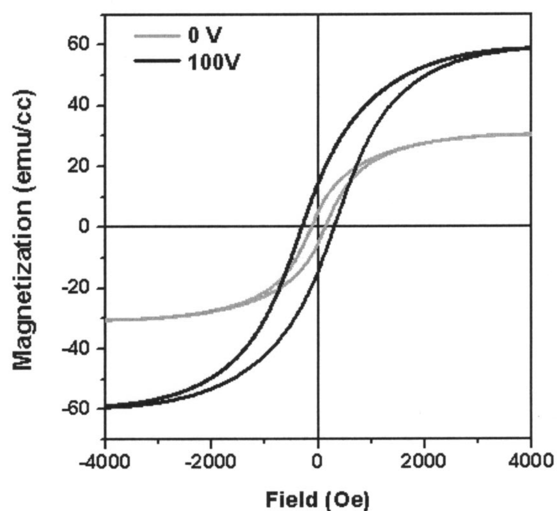

FIG. 5. Hysteresis loops of Fe_3O_4 thin films sputtered with and without substrate bias.

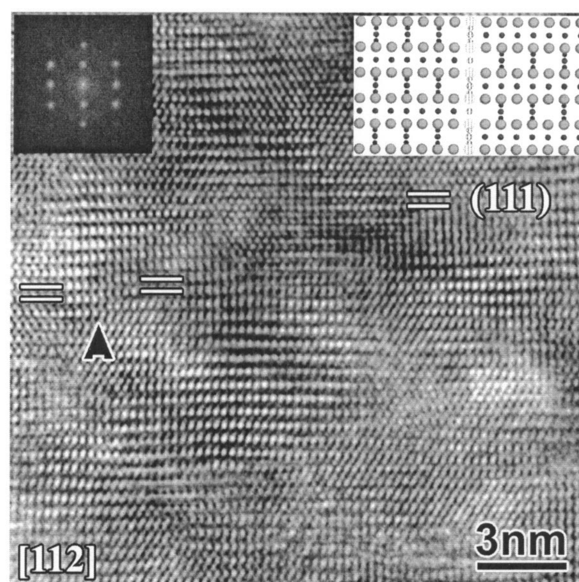

FIG. 6. High resolution TEM image showing typical defects in Fe_3O_4 grains. The inset at the upper-right corner is the [112] projection of the $(1\bar{1}0)$ antiphase boundary (APB) with $\frac{1}{4}[110]$ displacement, and one of that type of APB is indicated by an arrow.

crystallographic defects (antiphase boundaries) even in the bias sputtered thin films. A thin layer of amorphous boundary is also seen between the grains. The high density of defects might be due to the fact that the Fe_3O_4 phase formed is nonstoichiometrically and presumably Fe-poor. Though this could be part of the reason for the low M_s value we have obtained, the basic reason is still unclear.

ACKNOWLEDGMENTS

The authors gratefully acknowledge the Data Storage Systems Center for its financial support of the research project, and Professor Jian-Gang Zhu for discussions. Y.P. also thanks Dr. Shaoyan Chu for his help with SQUID measurements.

[1] D. M. Lind, S. M. Berry, G. Chern, H. Mathias, and L. R. Testardi, Phys. Rev. B **45**, 1838 (1992).
[2] C. A. Klient, H. C. Semmelhack, M. Lorenz, and M. K. Krause, J. Magn. Magn. Mater. **140–144**, 725 (1995).
[3] D. T. Margulies, F. T. Parker, F. E. Spada, R. S. Goldman, J. Li, R. Sinclair, and A. E. Berkowitz, Phys. Rev. B **53**, 9175 (1996).
[4] W. L. Zhou, K.-Y. Wang, C. J. O'Connor, and J. Tang, J. Appl. Phys. **89**, 7398 (2001).
[5] J. M. D. Coey, A. E. Berkowitz, L. I. Balcells, F. F. Putris, and F. T. Parker, Appl. Phys. Lett. **72**, 734 (1998).
[6] E. Lochner, K. A. Shaw, R. C. DiBari, W. Portwine, P. Stoyonov, S. D. Berry, and D. M. Lind, IEEE Trans. Magn. **30**, 4912 (1994).
[7] F. C. Voogt, T. Fujii, P. J. M. Smulders, L. Niesen, M. A. James, and T. Hibma, Phys. Rev. B **60**, 11193 (1999).
[8] T. S. Chin and N. C. Chiang, J. Appl. Phys. **81**, 5250 (1997).
[9] J. L. Labar, *Proceedings of EUREM 12*, 2000, Brno, edited by L. Frank and F. Ciampor (Czechoslovak Society for Electron Microscopy, Videmska, 2000), Vol. III, pp. 1379–380.
[10] S. B. Ogale, K. Ghosh, R. P. Sharma, R. L. Greene, R. Ramesh, and T. Venkatesan, Phys. Rev. B **57**, 7823 (1998).

Downloaded 23 May 2003 to 128.2.132.216. Redistribution subject to AIP license or copyright, see http://ojps.aip.org/japo/japcr.jsp